

# Electrically actuated Alq<sub>3</sub> nanospring arrays

G. D. Dice and M. J. Brett

Department of Electrical and Computer Engineering  
2nd Floor ECERF, University of Alberta  
Edmonton, Alberta, Canada, T6G 2V4  
grdice@ece.ualberta.ca

## ABSTRACT

We present an electrically controllable Fabry-Perot interferometer constructed from the organic material tris (8-hydroxyquinoline) aluminum (Alq<sub>3</sub>). Electrostatic compression of a two-turn helical Alq<sub>3</sub> nanospring film with a pitch of 300 nm deposited via glancing angle deposition (GLAD) between parallel, partially reflective mirrors controls the peak transmission wavelength. A 1.6 nm shift of the peak transmission wavelength from 582.4 nm to 580.8 nm is measured. The nanostructure provides the ability to electrically control the transmission wavelength of an optical filter.

**Keywords:** Fabry-Perot, nanospring, Alq<sub>3</sub>, GLAD, interferometer

## 1 INTRODUCTION

One feature that is desirable feature for optical filters is electrical control of the peak transmission wavelength. A shift of several nanometres will ideally result from a variable applied voltage. Fabry-Perot interferometry has previously been used to measure sub-nanometre length changes [1], to study the resonant frequencies of cantilever structures [2], for the creation of electromechanical motion transducers [3], and as the detection mechanism for chemical sensors constructed from porous silicon [4–6]. In this paper we discuss the fabrication and characterization of an electrically variable Fabry-Perot interferometer constructed from a porous, helically structured thin film of tris (8-hydroxyquinoline) aluminum (Alq<sub>3</sub>) deposited via glancing angle deposition (GLAD). The nanosprings are electrostatically compressed between two partially reflective mirrors. As the mirror separation is directly related to the peak transmission wavelength [7], the peak of the transmission band shifts to a shorter wavelength. In previous studies inorganic SiO<sub>2</sub>, which has a Young's modulus of  $\sim 90$  GPa, was used to create nanosprings [8], however, Alq<sub>3</sub> is much softer with a Young's modulus of  $\sim 2.3$  GPa [9]. As Alq<sub>3</sub> is softer than SiO<sub>2</sub>, the nanospring films experience nanometres of compression before device breakdown and demonstrate electrically variable optical behaviour. In this work, electrostatic compression results in a transmission band shift of  $\sim 1.6$  nm.

## 2 GLANCING ANGLE DEPOSITION

It is possible to create a number of optical filter devices such as rugate filters [10–12], chiral nanoengineered structures that selectively transmit circularly polarized light by utilizing the circular Bragg effect [13,14], anti-reflection coatings [15], humidity sensors [16], and photonic crystals [17] through the controlled single step deposition at glancing angles of incidence. GLAD is an advanced single step physical vapour deposition process where a porous thin film is created via a deposition angle of  $\alpha > 70^\circ$  relative to the substrate normal [18,19]. Thin film structures with specific architectures such as slanted posts, helices, vertical posts, and density-gradient columns may be grown with several nanometers of precision through deposition rate feedback. Alq<sub>3</sub> is an ideal material for use in a compressible nanospring device, as it produces low-defect nanospring structures [13], and has a Young's modulus that enables low voltage electrostatic compression.

## 3 NANOSPRING COMPRESSION

Previous work [8,20] determined that the spring constant of a compressible nanoscale helix can be calculated using the equation:

$$k = \frac{Yd^4}{128R^3n(1+\nu)} \left[ 1 - \frac{3d^2}{64R^2} + \frac{(3+\nu)}{2(1+\nu)} \tan^2(\alpha) \right] \quad (1)$$

where  $Y$  is the Young's modulus of the spring material,  $\nu$  is Poisson's ratio for the material,  $d$  is the diameter of the nanospring column,  $R$  is the coil radius,  $n$  is the number of turns, and  $\alpha$  is the spring pitch. For this spring constant, the nanospring deflection ( $\Delta x_s$ ) as a function of applied voltage for a parallel plate capacitor structure is determined by:

$$\Delta x_s = \frac{\epsilon_r \epsilon_0 A V_s^2}{h_s^2 i k} \quad (2)$$

where  $\epsilon_r$  is the dielectric constant of the filling material,  $i$  is the number of springs in the electrode area,  $A$  is the electrode area,  $V_s$  is portion of the applied voltage that drops across the nanosprings,  $h_s$  is the height

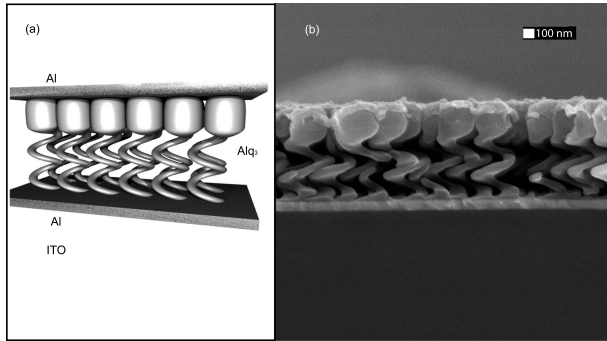


Figure 1: (a) Schematic depiction of the constructed nanostructure. (b) SEM image of the  $\text{Alq}_3$  nanospring structure. The helical pitch is 300 nm, with a 25 nm thick Al layer above and below the structure.

of the nanosprings, and  $k$  is the calculated spring constant. For the dense capping layer of the nanospring structure, the compression ( $\Delta x_c$ ) is calculated through:

$$\Delta x_c = \frac{\epsilon_r \epsilon_0 V_c^2}{Y h_c} \quad (3)$$

where  $V_c$  is the voltage that drops across the dense film layer, and  $h_c$  is the thickness of the layer [21]. The total compression of the nanospring structure is thus the sum of the individual compressions of each component. At a specific compression, the peak transmission wavelength of the Fabry-Perot interferometer will shift by:

$$\Delta \lambda = \frac{2\kappa}{m} \Delta x \quad (4)$$

where  $\Delta \lambda$  is the wavelength shift,  $\kappa$  is the effective refractive index of the nanospring structure, and  $m$  is the transmission mode of the Fabry-Perot [7].

#### 4 DEVICE CONSTRUCTION

Figure 1 (a) depicts a schematic diagram of the variable optical filter which shows that the device is constructed from three separate layers. The base layer of the transparent conductor indium tin oxide (ITO) provides a superior electrical path compared to the relatively thin mirror layers. A 25 nm thick aluminum layer forms a partially reflective mirror with  $\sim 80\%$  transmission, and one electrode of the parallel plate capacitor for electrostatic compression. A two-turn, right-handed helical  $\text{Alq}_3$  film with a 300 nm pitch is deposited on top of the reflective electrode via the GLAD PVD technique using a rotating substrate at a deposition angle of  $\alpha = 85^\circ$  via thermal evaporation. As the nanospring structure is highly porous, a solid capping layer of  $\text{Alq}_3$  deposited by decreasing the flux incidence angle  $\alpha$  during deposition [18]. A final 25 nm thick Aluminum film

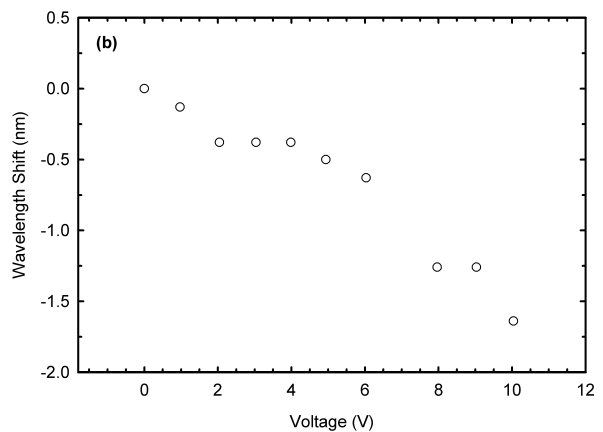
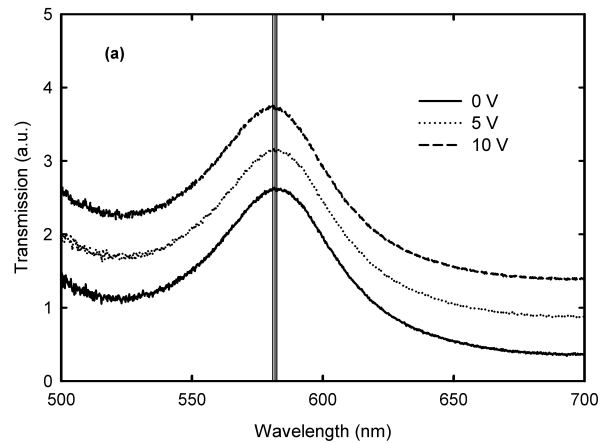


Figure 2: (a) (Solid Line) Transmission spectrum at 0 V. (dotted line) Transmission spectrum at 5 V. (dashed line) Transmission spectrum at 10 V. Spectra at 5 V and 10 V have been shifted along the transmission axis to better illustrate the wavelength shift. (b) (o) Shift in the peak wavelength of the transmission band a function of applied voltage from 0 V to 10 V.

is deposited and patterned with 3 mm  $\times$  3 mm electrodes to complete the device. Figure 1 (b) illustrates a SEM image of the edge of a completed device. The total device thickness is measured at  $\sim 790$  nm from the SEM image, with each helix having a column diameter of  $\sim 70$  nm.

The shift in the peak transmission wavelength as a function of applied voltage was measured using a fiber-coupled white light source shone at normal incidence onto the top partially reflective mirror. At each applied voltage a spherical lens focused light transmitted through the Fabry-Perot into a fiber-coupled spectrometer. Figure 2 (a) depicts the third mode of the transmission spectrum of the Fabry-Perot device at applied voltages of 0 V (solid line), 5 V (dotted line), and 10 V (dashed line). As the applied voltage compresses the

nanospring structure the transmission spectrum shifts to shorter wavelengths from an initial peak of 581 nm. Figure 2 (b) (o) illustrates that there is a measured shift in the peak transmission wavelength by 1.6 nm from 582.4 nm to 580.8 nm. This peak wavelength shift corresponds to a physical compression of 1.73 nm as the effective refractive index of the nanospring structure is  $\sim 1.42$  via the effective medium approximation [22].

We have demonstrated an electrically controlled Fabry-Perot interferometer based on a parallel plate capacitor structure filled with GLAD deposited nanosprings. A shift in the peak wavelength transmitted through the device results from electrostatic compression of the entire nanostructure. The ability to precisely control the transmission wavelength of an optical filter through an applied voltage is very useful for the creation of variable optical filter devices.

The authors gratefully acknowledge financial support from the Natural Sciences and Engineering Research Council of Canada (NSERC), Micralyne, Alberta Ingenuity, the NRC National Institute for Nanotechnology, and the Alberta Informatics Circle of Research Excellence (iCORE). The authors would also like to thank George D. Braybrook for the exceptional SEM imaging, and Mike Fleischauer for 3D graphics.

## REFERENCES

- [1] O. Cip, F. Petru, J. Lazar and Z. Buchta, *Ultra-precise measurement of distance by fabry-perot resonator*, *Phys. Scripta*, T118, 45–47, 2005.
- [2] P. M. Nieva, N. E. McGruer and G. G. Adams, *Design and characterization of a micromachined fabryperot vibration sensor for high-temperature applications*, *J. Micromech. Microeng.*, 16, 2618–2631, 2006.
- [3] R. L. Waters and M. E. Aklufi, *Micromachined fabryperot interferometer for motion detection*, *Appl. Phys. Lett.*, 81, 3320–3322, 2002.
- [4] C. L. Curtis, V. V. Doan, G. M. Credo and M. J. Sailor, *Observation of optical cavity modes in photoluminescent porous silicon films*, *J. Electrochem. Soc.*, 140, 3492–3494, 1993.
- [5] J. Gao, T. Gao and M. J. Sailor, *Porous-silicon vapor sensor based on laser interferometry*, *Appl. Phys. Lett.*, 77, 901–903, 2000.
- [6] A. Janshoff, K.-P. S. Dancil, C. Steinem, D. P. Greiner, V. S.-Y. Lin, C. Gurtner, K. Motesharei, M. J. Sailor and M. R. Ghadiri, *Macroporous p-type silicon fabry-perot layers. fabrication, characterization, and applications in biosensing*, *J. Am. Chem. Soc.*, 120, 12108–12116, 1998.
- [7] G. R. Fowles, *Introduction to modern optics*, New York, Holt, Rinehart, and Wilson, 1975.
- [8] M. W. Seto, K. Robbie, D. Vick, M. J. Brett and L. Kuhn, *Mechanical response of thin films with helical microstructures*, *J. Vac. Sci. Technol. B*, 17, 2172–2177, 1999.
- [9] Y. Cao, C. Kim, S. R. Forrest and W. Soboyejo, *Effects of dust particles and layer properties on organic electronic devices fabricated by stamping*, *J. Appl. Phys.*, 98, 033713, 2005.
- [10] M. M. Hawkeye and M. J. Brett, *Narrow bandpass optical filters fabricated with one-dimensionally periodic inhomogeneous thin films*, *J. Appl. Phys.*, 100, 044322, 2006.
- [11] K. Robbie, A. J. P. Hnatiw, M. J. Brett, R. I. MacDonald and J. N. McMullin, *Inhomogeneous thin film optical filters fabricated using glancing angle deposition*, *Electron. Lett.*, 33, 1213–1214, 1997.
- [12] A. C. van Popta, M. M. Hawkeye, J. C. Sit and M. J. Brett, *Gradient-index narrow-bandpass filter fabricated with glancing-angle deposition*, *Opt. Lett.*, 29, 2545–2547, 2004.
- [13] P. C. P. Hruday, K. L. Westra and M. J. Brett, *Highly ordered organic Alq<sub>3</sub> chiral luminescent thin films fabricated by glancing-angle deposition*, *Adv. Mater.*, 18, 224–228, 2005.
- [14] P. C. P. Hruday, M. Taschuk, Y. Y. Tsui, R. Fedosejevs and M. J. Brett, *Optical properties of porous nanostructured Y<sub>2</sub>O<sub>3</sub>:Eu thin films*, *J. Vac. Sci. Technol. A*, 23, 856–861, 2005.
- [15] S. R. Kennedy and M. J. Brett, *Porous broadband antireflection coating by glancing angle deposition*, *Appl. Opt.*, 42, 4573–4579, 2003.
- [16] J. J. Steele, J. P. Gospodyn, J. C. Sit and M. J. Brett, *Impact of morphology on high-speed humidity sensor performance*, *IEEE Sens J*, 6, 24–27, 2006.
- [17] S. R. Kennedy, M. J. Brett, O. Toader and S. John, *Fabrication of tetragonal square spiral photonic crystals*, *Nano. Lett.*, 2, 59–62, 2002.
- [18] K. Robbie and M. J. Brett, *Sculptured thin films and glancing angle deposition: Growth mechanics and applications*, *J. Vac. Sci. Technol. A*, 15, 1460–1465, 1997.
- [19] K. Robbie, M. J. Brett and A. Lakhtakia, *Chiral sculptured thin films*, *Nature*, 384, 616, 1996.
- [20] M. W. Seto, B. Dick and M. J. Brett, *Microsprings and microcantilevers: studies of mechanical response*, *J. Micromech. Microeng.*, 11, 582–588, 2001.
- [21] D. Halliday, R. Resnick and J. Walker, *Fundamentals of Physics: Sixth Edition*, New York, John Wiley & Sons, Inc., 2001.
- [22] T. C. Choy, *Effective medium theory : principles and applications*, New York, Oxford University Press, 1999.